

Nature of light scalars through photon-photon collisions^{*}

N. N. Achasov¹⁾ G. N. Shestakov²⁾

Laboratory of Theoretical Physics, Sobolev Institute for Mathematics, Novosibirsk, 630090, Russia

Abstract The surprising thing is that arising almost 50 years ago from the linear sigma model (LSM) with spontaneously broken chiral symmetry, the light scalar meson problem has become central in the nonperturbative quantum chromodynamics (QCD) for it has been made clear that LSM could be the low energy realization of QCD. First we review briefly signs of four-quark nature of light scalars. Then we show that the light scalars are produced in the two photon collisions via four-quark transitions in contrast to the classic P wave tensor $q\bar{q}$ mesons that are produced via two-quark transitions $\gamma\gamma \rightarrow q\bar{q}$. Thus we get new evidence of the four-quark nature of these states.

Key words linear sigma model, light scalar mesons, four-quark states, two photon production mechanisms

PACS 12.39.-x, 13.40.-f, 13.60.Le

1 Introduction

The scalar channels in the region up to 1 GeV became a stumbling block of QCD. The point is that both perturbation theory and sum rules do not work in these channels because there are not solitary resonances in this region. At the same time the question on the nature of the light scalar mesons is major for understanding the mechanism of the chiral symmetry realization, arising from the confinement, and hence for understanding the confinement itself.

2 QCD, chiral limit, confinement, σ -models

$L = -(1/2)\text{Tr}(G_{\mu\nu}(x)G^{\mu\nu}(x)) + \bar{q}(x)(i\hat{D} - M)q(x)$. M mixes left and right spaces $q_L(x)$ and $q_R(x)$. But in chiral limit $M \rightarrow 0$ these spaces separate realizing $U_L(3) \times U_R(3)$ flavour symmetry. Experiment suggests, confinement forms colourless observable hadronic fields and spontaneous breaking of chiral symmetry with massless pseudoscalar fields. There are two possible scenarios for QCD at low energy. 1) $U_L(3) \times U_R(3)$ non-linear σ -model. 2) $U_L(3) \times U_R(3)$ linear σ -model. The experimental nonet

of the light scalar mesons suggests $U_L(3) \times U_R(3)$ linear σ -model.

3 History of light scalar mesons

Hunting the light σ and κ mesons had begun in the sixties already. But long-standing unsuccessful attempts to prove their existence in a conclusive way entailed general disappointment and an information on these states disappeared from PDG Reviews. One of principal reasons against the σ and κ mesons was the fact that both $\pi\pi$ and πK scattering phase shifts do not pass over 90° at putative resonance masses. [Meanwhile, there were discovered the narrow light scalar resonances, the isovector $a_0(980)$ and isoscalar $f_0(980)$.]

4 $SU_L(2) \times SU_R(2)$ linear σ -model [1]

Situation changes when we showed that in the linear σ -model

$$L = \frac{1}{2}[(\partial_\mu \sigma)^2 + (\partial_\mu \vec{\pi})^2] - \frac{m_\sigma^2}{2}\sigma^2 - \frac{m_\pi^2}{2}\vec{\pi}^2 - \frac{m_\sigma^2 - m_\pi^2}{8f_\pi^2}[(\sigma^2 + \vec{\pi}^2)^2 + 4f_\pi\sigma(\sigma^2 + \vec{\pi}^2)]^2,$$

Received 26 January 2010

^{*} Supported by RFFI Grant No. 07-02-00093 from the Russian Foundation for Basic Research and Presidential Grant No. NSh-1027.2008.2 for Leading Scientific Schools

1) E-mail: achasov@math.nsc.ru

2) E-mail: shestako@math.nsc.ru

©2009 Chinese Physical Society and the Institute of High Energy Physics of the Chinese Academy of Sciences and the Institute of Modern Physics of the Chinese Academy of Sciences and IOP Publishing Ltd

there is a negative background phase which hides the σ meson. It has been made clear that shielding wide lightest scalar mesons in chiral dynamics is very natural. This idea was picked up and triggered new wave of theoretical and experimental searches for the σ and κ mesons.

5 Our approximation [1, 2]

Our approximation is as follows (see Fig. 1):

$$T_0^{0(\text{tree})} = \frac{m_\pi^2 - m_\sigma^2}{32\pi f_\pi^2} \left[5 - 3 \frac{m_\sigma^2 - m_\pi^2}{m_\sigma^2 - s} - 2 \frac{m_\sigma^2 - m_\pi^2}{s - 4m_\pi^2} \ln \left(1 + \frac{s - 4m_\pi^2}{m_\sigma^2} \right) \right],$$

$$T_0^0 = \frac{T_0^{0(\text{tree})}}{1 - i\rho_{\pi\pi} T_0^{0(\text{tree})}} = \frac{e^{2i(\delta_{\text{res}} + \delta_{\text{bg}})} - 1}{2i\rho_{\pi\pi}} = \frac{e^{2i\delta_0^0} - 1}{2i\rho_{\pi\pi}} = T_{\text{bg}} + e^{2i\delta_{\text{bg}}} T_{\text{res}},$$

$$T_{\text{bg}} = \frac{e^{2i\delta_{\text{bg}}} - 1}{2i\rho_{\pi\pi}}, \quad T_{\text{res}} = \frac{e^{2i\delta_{\text{res}}} - 1}{2i\rho_{\pi\pi}},$$

$$T_{\text{bg}} = \frac{\lambda(s)}{1 - i\rho_{\pi\pi}\lambda(s)}, \quad \rho_{\pi\pi} = \sqrt{1 - \frac{4m_\pi^2}{s}},$$

$$\lambda(s) =$$

$$\frac{m_\pi^2 - m_\sigma^2}{32\pi f_\pi^2} \left[5 - 2 \frac{m_\sigma^2 - m_\pi^2}{s - 4m_\pi^2} \ln \left(1 + \frac{s - 4m_\pi^2}{m_\sigma^2} \right) \right],$$

$$T_{\text{res}} = \frac{1}{\rho_{\pi\pi}} \cdot \frac{\sqrt{s} \Gamma_{\text{res}}(s)}{M_{\text{res}}^2 - s + \text{Re} \Pi_{\text{res}}(M_{\text{res}}^2) - \Pi_{\text{res}}(s)},$$

$$M_{\text{res}}^2 = m_\sigma^2 - \text{Re} \Pi_{\text{res}}(M_{\text{res}}^2),$$

$$\text{Im} \Pi_{\text{res}}(s) = \sqrt{s} \Gamma_{\text{res}}(s) = \frac{g_{\text{res}}^2(s)}{16\pi} \rho_{\pi\pi},$$

$$\text{Re} \Pi_{\text{res}}(s) = -\frac{g_{\text{res}}^2(s)}{16\pi} \lambda(s) \rho_{\pi\pi}^2,$$

$$g_{\text{res}}(s) = \frac{g_{\sigma\pi\pi}}{|1 - i\rho_{\pi\pi}\lambda(s)|},$$

$$g_{\sigma\pi\pi} = \sqrt{3/2} g_{\sigma\pi^+\pi^-}, \quad g_{\sigma\pi^+\pi^-} = (m_\pi^2 - m_\sigma^2)/f_\pi,$$

$$T_0^2 = \frac{T_0^{2(\text{tree})}}{1 - i\rho_{\pi\pi} T_0^{2(\text{tree})}} = \frac{e^{2i\delta_0^2} - 1}{2i\rho_{\pi\pi}},$$

$$T_0^{2(\text{tree})} =$$

$$\frac{m_\pi^2 - m_\sigma^2}{32\pi f_\pi^2} \left[2 - 2 \frac{m_\sigma^2 - m_\pi^2}{s - 4m_\pi^2} \ln \left(1 + \frac{s - 4m_\pi^2}{m_\sigma^2} \right) \right].$$

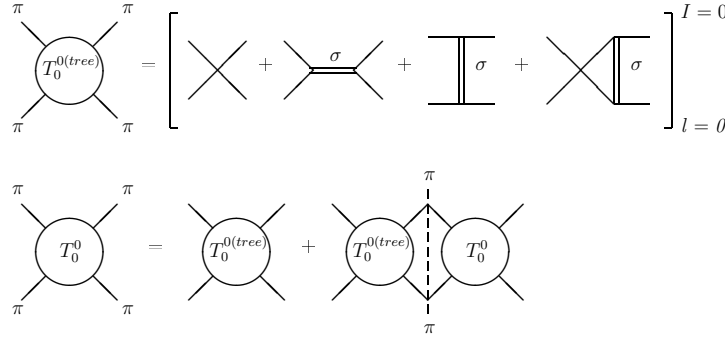


Fig. 1. The graphical representation of the S wave $I=0$ $\pi\pi$ scattering amplitude T_0^0 .

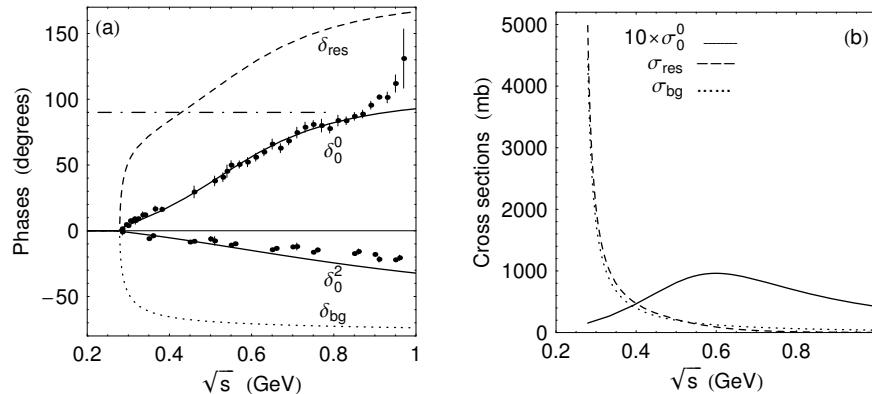


Fig. 2. The σ model. Our approximation.

6 Chiral shielding in $\pi\pi \rightarrow \pi\pi$ [1, 2]

The results in our approximation are: $M_{\text{res}} = 0.43$ GeV, $\Gamma_{\text{res}}(M_{\text{res}}^2) = 0.67$ GeV, $m_\sigma = 0.93$ GeV,

$$\Gamma_{\text{res}}^{\text{renorm}}(M_{\text{res}}^2) = \frac{\Gamma_{\text{res}}(M_{\text{res}}^2)}{1 + d[\text{Re}\Pi_{\text{res}}(s)]/ds} \Big|_{s=M_{\text{res}}^2} = 0.53 \text{ GeV},$$

$g_{\text{res}}(M_{\text{res}}^2)/g_{\sigma\pi\pi} = 0.33$, $a_0^0 = 0.18 m_\pi^{-1}$, $a_0^2 = -0.04 m_\pi^{-1}$, the Adler zeros $(s_A)_0^0 = 0.45 m_\pi^2$ and $(s_A)_0^2 = 2.02 m_\pi^2$.

The chiral shielding of the $\sigma(600)$ meson in $\pi\pi \rightarrow \pi\pi$ is illustrated in Fig. 2 with the help of the $\pi\pi$ phase shifts δ_{res} , δ_{bg} , $\delta_0^0 = \delta_{\text{res}} + \delta_{\text{bg}}$ (a), and with the help of the corresponding cross sections (b).

7 The σ pole and σ propagator [2]

In the pole $T_0^0 \rightarrow g_\pi^2/(s - s_R)$, where $g_\pi^2 = (0.12 + i0.21)$ GeV², $s_R = (0.21 - i0.26)$ GeV², $\sqrt{s_R} = M_R - i\Gamma_R/2 = (0.52 - i0.25)$ GeV. Considering the residue of

the σ pole in T_0^0 as the square of its coupling constant to the $\pi\pi$ channel is not a clear guide to understand the σ meson nature for its great obscure imaginary part.

Another matter the σ meson propagator

$$\frac{1}{D_\sigma(s)} = \frac{1}{M_{\text{res}}^2 - s + \text{Re}\Pi_{\text{res}}(M_{\text{res}}^2) - \Pi_{\text{res}}(s)}.$$

The σ meson self-energy $\Pi_{\text{res}}(s)$ is caused by the intermediate $\pi\pi$ states, that is, by the four-quark intermediate states. This contribution shifts the Breit-Wigner (BW) mass greatly $m_\sigma - M_{\text{res}} = 0.50$ GeV. So, half the BW mass is determined by the four-quark contribution at least. The imaginary part dominates the propagator modulus in the region $300 \text{ MeV} < \sqrt{s} < 600 \text{ MeV}$. So, the σ field is described by its four-quark component at least in this energy (virtuality) region.

8 Chiral shielding in $\gamma\gamma \rightarrow \pi\pi$ [2]

The $\gamma\gamma \rightarrow \pi^+\pi^-$ reaction amplitude is given by

$$T_S(\gamma\gamma \rightarrow \pi^+\pi^-) = T_S^{\text{Born}}(\gamma\gamma \rightarrow \pi^+\pi^-) + 8\alpha I_{\pi^+\pi^-} \times T_S(\pi^+\pi^- \rightarrow \pi^+\pi^-) = [T_S^{\text{Born}}(\gamma\gamma \rightarrow \pi^+\pi^-) + 8\alpha I_{\pi^+\pi^-} \times (2T_0^0 + T_0^2)/3] \text{ in elastic region} = \frac{2}{3} e^{i\delta_0^0} \left\{ T_S^{\text{Born}}(\gamma\gamma \rightarrow \pi^+\pi^-) \cos \delta_0^0 + \frac{8\alpha}{\rho_{\pi\pi}} (\text{Re}I_{\pi^+\pi^-}) \sin \delta_0^0 \right\} + \frac{1}{3} e^{i\delta_0^2} \left\{ T_S^{\text{Born}}(\gamma\gamma \rightarrow \pi^+\pi^-) \cos \delta_0^2 + \frac{8\alpha}{\rho_{\pi\pi}} (\text{Re}I_{\pi^+\pi^-}) \sin \delta_0^2 \right\}.$$

The $\gamma\gamma \rightarrow \pi^0\pi^0$ reaction amplitude is given by $T_S(\gamma\gamma \rightarrow \pi^0\pi^0) = 8\alpha I_{\pi^+\pi^-} T_S(\pi^+\pi^- \rightarrow \pi^+\pi^-) = 16\alpha \times I_{\pi^+\pi^-} (T_0^0 - T_0^2)/3$ in elastic region =

$$\frac{2}{3} e^{i\delta_0^0} \left\{ T_S^{\text{Born}}(\gamma\gamma \rightarrow \pi^+\pi^-) \cos \delta_0^0 + \frac{8\alpha}{\rho_{\pi\pi}} (\text{Re}I_{\pi^+\pi^-}) \sin \delta_0^0 \right\} - \frac{2}{3} e^{i\delta_0^2} \left\{ T_S^{\text{Born}}(\gamma\gamma \rightarrow \pi^+\pi^-) \cos \delta_0^2 + \frac{8\alpha}{\rho_{\pi\pi}} (\text{Re}I_{\pi^+\pi^-}) \sin \delta_0^2 \right\}.$$

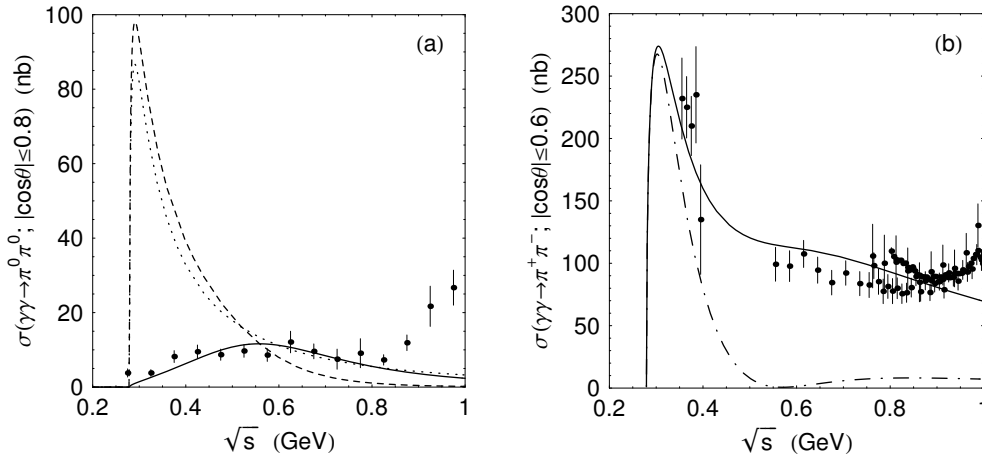


Fig. 3. (a) The solid, dashed, and dotted lines are $\sigma_S(\gamma\gamma \rightarrow \pi^0\pi^0)$, $\sigma_{\text{res}}(\gamma\gamma \rightarrow \pi^0\pi^0)$, and $\sigma_{\text{bg}}(\gamma\gamma \rightarrow \pi^0\pi^0)$. (b) The dashed-dotted line is $\sigma_S(\gamma\gamma \rightarrow \pi^+\pi^-)$. The solid line includes the higher waves from $T^{\text{Born}}(\gamma\gamma \rightarrow \pi^+\pi^-)$.

Here $T_S^{\text{Born}}(\gamma\gamma \rightarrow \pi^+\pi^-) = (8\alpha/\rho_{\pi\pi})\text{Im}I_{\pi^+\pi^-}$, $\alpha = 1/137$, and the triangle $\pi^+\pi^-$ loop integral

$$I_{\pi^+\pi^-} = \frac{m_\pi^2}{s} \left(\pi + i \ln \frac{1 + \rho_{\pi\pi}}{1 - \rho_{\pi\pi}} \right)^2 - 1,$$

for $s \geq 4m_\pi^2$.

Figure 3 illustrates the chiral shielding of the $\sigma(600)$ in the cross sections $\gamma\gamma \rightarrow \pi\pi$.

9 Four-quark transition $\sigma \rightarrow \gamma\gamma$ [2]

The energy dependent $\sigma \rightarrow \gamma\gamma$ decay width

$$\Gamma(\sigma \rightarrow \pi^+\pi^- \rightarrow \gamma\gamma, s) = \frac{1}{16\pi\sqrt{s}} |g(\sigma \rightarrow \pi^+\pi^- \rightarrow \gamma\gamma, s)|^2,$$

where

$$g(\sigma \rightarrow \pi^+\pi^- \rightarrow \gamma\gamma, s) = (\alpha/2\pi) I_{\pi^+\pi^-} g_{\text{res } \pi^+\pi^-}(s),$$

is shown in Fig. 4.

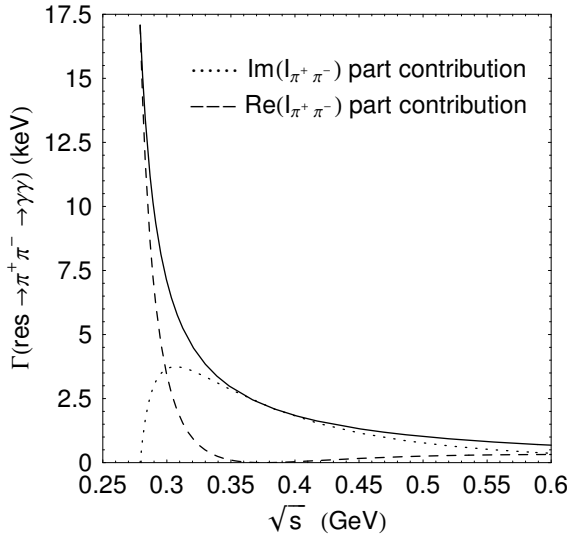


Fig. 4. The $\sigma \rightarrow \gamma\gamma$ decay width.

So, the the $\sigma \rightarrow \gamma\gamma$ decay is described by the triangle $\pi^+\pi^-$ loop diagram $\text{res} \rightarrow \pi^+\pi^- \rightarrow \gamma\gamma$ ($I_{\pi^+\pi^-}$). Consequently, it is due to the four-quark transition because we imply a low energy realization of the two-flavour QCD by means of the the $SU_L(2) \times SU_R(2)$ linear σ -model. As the Fig. 4 suggests, the real intermediate $\pi^+\pi^-$ state dominates in $g(\text{res} \rightarrow \pi^+\pi^- \rightarrow \gamma\gamma)$ in the σ region $\sqrt{s} < 0.6$ GeV. Thus the picture in the physical region is clear and informative. But, what about the pole in the complex s -plane? Does the pole residue reveal the σ indeed?

In the σ pole for $\gamma\gamma \rightarrow \pi\pi$ one has

$$\frac{1}{16\pi} \sqrt{\frac{3}{2}} T_S(\gamma\gamma \rightarrow \pi^0\pi^0) \rightarrow g_\gamma g_\pi / (s - s_R),$$

$g_\gamma g_\pi = (-0.45 - i0.19) \times 10^{-3} \text{ GeV}^2$, $g_\gamma/g_\pi = (-1.61 + i1.21) \times 10^{-3}$, $\Gamma(\sigma \rightarrow \gamma\gamma) = |g_\gamma|^2/M_R \approx 2 \text{ keV}$. It is hard to believe that anybody could learn the complex but physically clear dynamics of the $\sigma \rightarrow \gamma\gamma$ decay described above from the residues of the σ pole.

10 First lessons

1) Leutwyler and collaborators [3] obtained

$$\sqrt{s_R} = M_R - i\Gamma_R/2 = (441_{-8}^{+16} - i272_{-9}^{+12.5}) \text{ MeV}$$

with the help of the Roy equation. Our result agrees with the above qualitatively

$$\sqrt{s_R} = M_R - i\Gamma_R/2 = (518 - i250) \text{ MeV}.$$

2) Could the above scenario incorporates the primary lightest scalar Jaffe four-quark state [4]? Certainly the direct coupling of this state to $\gamma\gamma$ via neutral vector pairs ($\rho^0\rho^0$ and $\omega\omega$), contained in its wave function, is negligible $\Gamma(q^2\bar{q}^2 \rightarrow \rho^0\rho^0 + \omega\omega \rightarrow \gamma\gamma) \approx 10^{-3} \text{ keV}$ as we showed in 1982 [5]. But its coupling to $\pi\pi$ is strong and leads to $\Gamma(q^2\bar{q}^2 \rightarrow \pi^+\pi^- \rightarrow \gamma\gamma)$ similar to $\Gamma(\text{res} \rightarrow \pi^+\pi^- \rightarrow \gamma\gamma)$ in the above Fig. 4. Let us add to $T_S(\gamma\gamma \rightarrow \pi^0\pi^0)$ the amplitude for the the direct coupling of σ to $\gamma\gamma$ conserving unitarity

$$T_{\text{direct}}(\gamma\gamma \rightarrow \pi^0\pi^0) = s g_{\sigma\gamma\gamma}^{(0)} g_{\text{res}}(s) e^{i\delta_{b\pi}} / D_{\text{res}}(s),$$

where $g_{\sigma\gamma\gamma}^{(0)}$ is the direct coupling constant of σ to $\gamma\gamma$, the factor s is caused by gauge invariance. Fitting the $\gamma\gamma \rightarrow \pi^0\pi^0$ data gives a negligible value of $g_{\sigma\gamma\gamma}^{(0)}$, $\Gamma_{\sigma\gamma\gamma}^{(0)} = |M_{\text{res}}^2 g_{\sigma\gamma\gamma}^{(0)}|^2 / (16\pi M_{\text{res}}) \approx 0.0034 \text{ keV}$, in astonishing agreement with our old prediction [5].

3) The majority of current investigations of the mass spectra in scalar channels does not study particle production mechanisms. That is why such investigations are only preprocessing experiments, and the derivable information is very relative. The only progress in understanding the particle production mechanisms could essentially advance us in revealing the light scalar meson nature, as is evident from the foregoing.

11 Troubles and expectancies

In theory the principal problem is impossibility to use the linear σ -model in the tree level approximation inserting widths into σ meson propagators because such an approach breaks both the unitarity and the Adler self-consistency conditions. The comparison with the experiment requires the non-perturbative calculation of the process amplitudes. Nevertheless, now there are the possibilities to estimate odds of

the $U_L(3) \times U_R(3)$ linear σ -model to underlie physics of light scalar mesons in phenomenology, taking into account the idea of chiral shielding, our treatment of $\sigma(600)$ - $f_0(980)$ mixing based on quantum field theory ideas, and Adler's conditions [6].

An example of the phenomenological treatment is shown in Fig. 5 with $g_{\sigma\pi^+\pi^-}^2/4\pi = 0.99 \text{ GeV}^2$, $g_{\sigma K^+K^-}^2/4\pi = 2 \cdot 10^{-4} \text{ GeV}^2$, $g_{f_0\pi^+\pi^-}^2/4\pi = 0.12 \text{ GeV}^2$, $g_{f_0K^+K^-}^2/4\pi = 1.04 \text{ GeV}^2$, $m_\sigma = 679 \text{ MeV}$, $\Gamma_\sigma = 498 \text{ MeV}$, $m_{f_0} = 989 \text{ MeV}$, and the $J=I=0$ $\pi\pi$ scattering length $a_0^0 = 0.223 m_{\pi^+}^{-1}$.

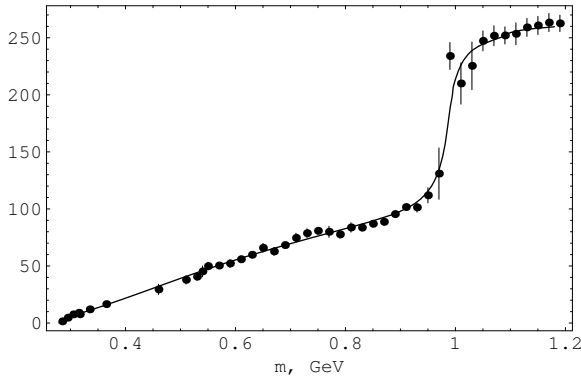


Fig. 5. The $\pi\pi$ phase shift $\delta_0^0 = \delta_B^{\pi\pi} + \delta_{\text{res}}$.

12 Four-quark model

The nontrivial nature of the well-established light scalar resonances $f_0(980)$ and $a_0(980)$ is no longer denied practically anybody. As for the nonet as a whole, even a cursory look at PDG Review gives an idea of the four-quark structure of the light scalar meson nonet, $\sigma(600)$, $\kappa(800)$, $f_0(980)$, and $a_0(980)$, inverted in comparison with the classical P wave $q\bar{q}$ tensor meson nonet $f_2(1270)$, $a_2(1320)$, $K_2^*(1420)$, $f_2'(1525)$. Really, while the scalar nonet cannot be treated as the P wave $q\bar{q}$ nonet in the naive quark model, it can

be easy understood as the $q^2\bar{q}^2$ nonet, where σ has no strange quarks, κ has the s quark, f_0 and a_0 have the $s\bar{s}$ pair. Similar states were found by Jaffe in 1977 in the MIT bag [4].

13 Radiative decays of ϕ meson [7]

Ten years later we showed that $\phi \rightarrow \gamma a_0 \rightarrow \gamma\pi\pi$ and $\phi \rightarrow \gamma f_0 \rightarrow \gamma\pi\pi$ can shed light on the problem of $a_0(980)$ and $f_0(980)$ mesons. Now these decays are studied not only theoretically but also experimentally. The measurements (1998, 2000) were reported by SND and CMD-2. After (2002) they were studied by KLOE in agreement with the Novosibirsk data but with a considerably smaller error. Note that $a_0(980)$ is produced in the radiative ϕ meson decay as intensively as $\eta'(958)$ containing $\approx 66\%$ of $s\bar{s}$, responsible for $\phi \approx s\bar{s} \rightarrow \gamma s\bar{s} \rightarrow \gamma\eta'(958)$. It is a clear qualitative argument for the presence of the $s\bar{s}$ pair in the isovector $a_0(980)$ state, i.e., for its four-quark nature.

14 K^+K^- loop model [7]

When basing the experimental investigations, we suggested one-loop model $\phi \rightarrow K^+K^- \rightarrow \gamma a_0/f_0$, see Fig. 6. This model is used in the data treatment and is ratified by experiment, see Fig. 7. Gauge invariance gives the conclusive arguments in favor of the K^+K^- loop transition as the principal mechanism of $a_0(980)$ and $f_0(980)$ meson production in the ϕ radiative decays.

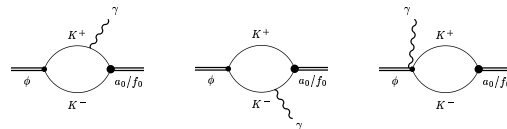


Fig. 6. The K^+K^- loop model.

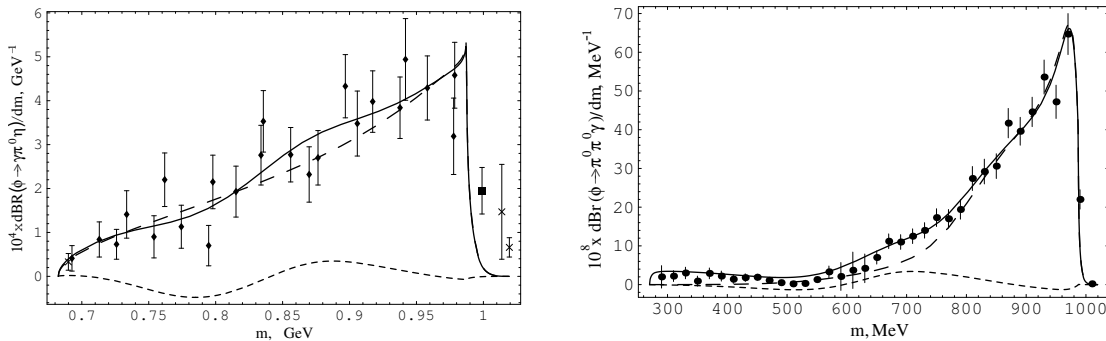


Fig. 7. The left (right) plot shows the fit to the KLOE data for the $\pi^0\eta$ ($\pi^0\pi^0$) mass spectrum in the $\phi \rightarrow \gamma\pi^0\eta$ ($\phi \rightarrow \gamma\pi^0\pi^0$) decay caused by the $a_0(980)$ ($\sigma(600)+f_0(980)$) production through the K^+K^- loop mechanism.

15 K^+K^- loop mechanism is established [7]

In truth this means that $a_0(980)$ and $f_0(980)$ are seen in the radiative decays of ϕ meson owing to K^+K^- intermediate state. So, the mechanism of production of $a_0(980)$ and $f_0(980)$ mesons in the ϕ radiative decays is established at a physical level of proof. We are dealing with the the four-quark transition. A radiative four-quark transition between two $q\bar{q}$ states requires creation and annihilation of an additional $q\bar{q}$ pair, i.e., such a transition is forbidden according to the OZI rule, while a radiative four-quark transition between $q\bar{q}$ and $q^2\bar{q}^2$ states requires only creation of an additional $q\bar{q}$ pair, i.e., such a transition is allowed according to the OZI rule. The large N_C expansion supports this conclusion.

16 $a_0(980)/f_0(980) \rightarrow \gamma\gamma$ & $q^2\bar{q}^2$ model [5, 8]

Twenty seven years ago we predicted the suppression of $a_0(980) \rightarrow \gamma\gamma$ and $f_0(980) \rightarrow \gamma\gamma$ in the $q^2\bar{q}^2$ MIT model [5],

$$\Gamma(a_0(980) \rightarrow \gamma\gamma) \sim \Gamma(f_0(980) \rightarrow \gamma\gamma) \sim 0.27 \text{ keV.}$$

Experiment supported this prediction $\Gamma(a_0 \rightarrow \gamma\gamma) = (0.19 \pm 0.07_{-0.07}^{+0.1})/B(a_0 \rightarrow \pi\eta) \text{ keV}$, Crystal Ball, $\Gamma(a_0 \rightarrow \gamma\gamma) = (0.28 \pm 0.04 \pm 0.1)/B(a_0 \rightarrow \pi\eta) \text{ keV}$, JADE, $\Gamma(f_0 \rightarrow \gamma\gamma) = (0.31 \pm 0.14 \pm 0.09) \text{ keV}$, Crystal Ball, $\Gamma(f_0 \rightarrow \gamma\gamma) = (0.24 \pm 0.06 \pm 0.15) \text{ keV}$, MARK II.

When in the $q\bar{q}$ model it was anticipated $\Gamma(a_0 \rightarrow \gamma\gamma) = (1.5 - 5.9)\Gamma(a_2 \rightarrow \gamma\gamma) = (1.5 - 5.9)(1.04 \pm 0.09) \text{ keV}$, $\Gamma(f_0 \rightarrow \gamma\gamma) = (1.7 - 5.5)\Gamma(f_2 \rightarrow \gamma\gamma) = (1.7 - 5.5)(2.8 \pm 0.4) \text{ keV}$.

17 Scalar nature and production mechanisms in $\gamma\gamma$ collisions [9]

Recently the experimental investigations have made great qualitative advance. The Belle Collaboration published data on $\gamma\gamma \rightarrow \pi^+\pi^-$ (2007), $\gamma\gamma \rightarrow \pi^0\pi^0$ (2008), and $\gamma\gamma \rightarrow \pi^0\eta$ (2009), whose statistics are huge [10]. They not only proved the theoretical expectations based on the four-quark nature of the light scalar mesons, but also have allowed to elucidate the principal mechanisms of these processes. Specifically, the direct coupling constants of the $\sigma(600)$, $f_0(980)$, and $a_0(980)$ resonances with the $\gamma\gamma$ system are small with the result that their decays in the two photon are the four-quark transitions caused by the rescatterings $\sigma \rightarrow \pi^+\pi^- \rightarrow \gamma\gamma$, $f_0(980) \rightarrow K^+K^- \rightarrow \gamma\gamma$ and $a_0(980) \rightarrow K^+K^- \rightarrow \gamma\gamma$ in contrast to the two-photon decays of the classic P wave tensor $q\bar{q}$ mesons $a_2(1320)$, $f_2(1270)$ and $f_2'(1525)$, which are caused by the direct two-quark transitions $q\bar{q} \rightarrow \gamma\gamma$ in the main. As a result the practically model-independent prediction of the $q\bar{q}$ model $g_{f_2\gamma\gamma}^2 : g_{a_2\gamma\gamma}^2 = 25 : 9$ agrees with experiment rather well. The two-photon light scalar widths averaged over resonance mass distributions $\langle \Gamma_{f_0 \rightarrow \gamma\gamma} \rangle_{\pi\pi} \approx 0.19 \text{ keV}$, $\langle \Gamma_{a_0 \rightarrow \gamma\gamma} \rangle_{\pi\pi} \approx 0.34 \text{ keV}$ and $\langle \Gamma_{\sigma \rightarrow \gamma\gamma} \rangle_{\pi\pi} \approx 0.45 \text{ keV}$. As to the ideal $q\bar{q}$ model prediction $g_{f_0\gamma\gamma}^2 : g_{a_0\gamma\gamma}^2 = 25 : 9$, it is excluded by experiment.

18 Dynamics of $\gamma\gamma \rightarrow \pi^+\pi^-$, $\gamma\gamma \rightarrow \pi^0\pi^0$ and $\gamma\gamma \rightarrow \pi^0\eta$ [9]

The following figures give a scetch of our treatment of the Belle data on the reactions $\gamma\gamma \rightarrow \pi\pi$ and $\gamma\gamma \rightarrow \pi^0\eta$.

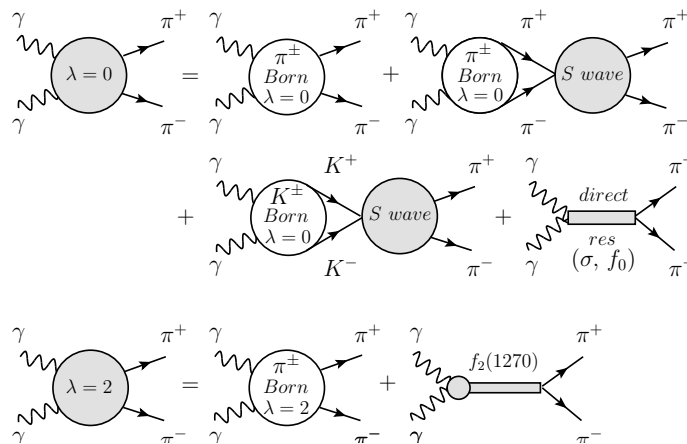


Fig. 8. Diagrammatical representation for the helicity amplitudes $\gamma\gamma \rightarrow \pi^+\pi^-$.

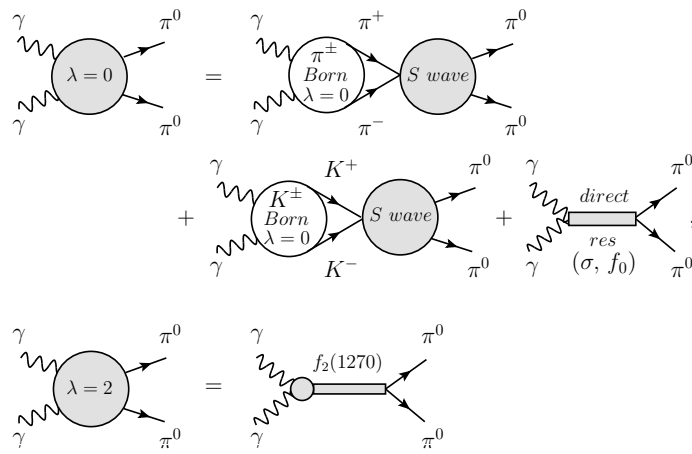


Fig. 9. Diagrammatic representation for the helicity amplitudes $\gamma\gamma \rightarrow \pi^0\pi^0$.

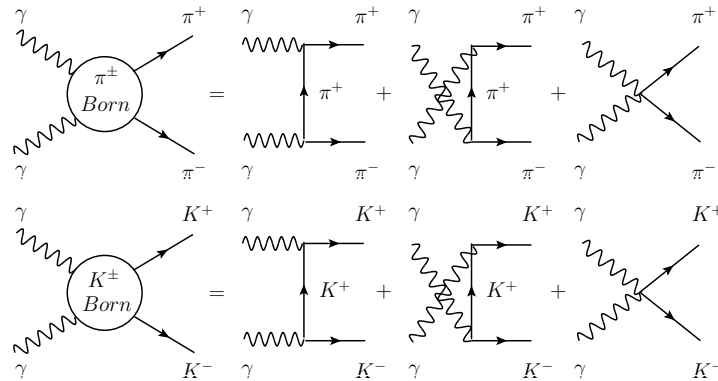


Fig. 10. The Born sources for $\gamma\gamma \rightarrow \pi^+\pi^-$ and $\gamma\gamma \rightarrow K^+K^-$.

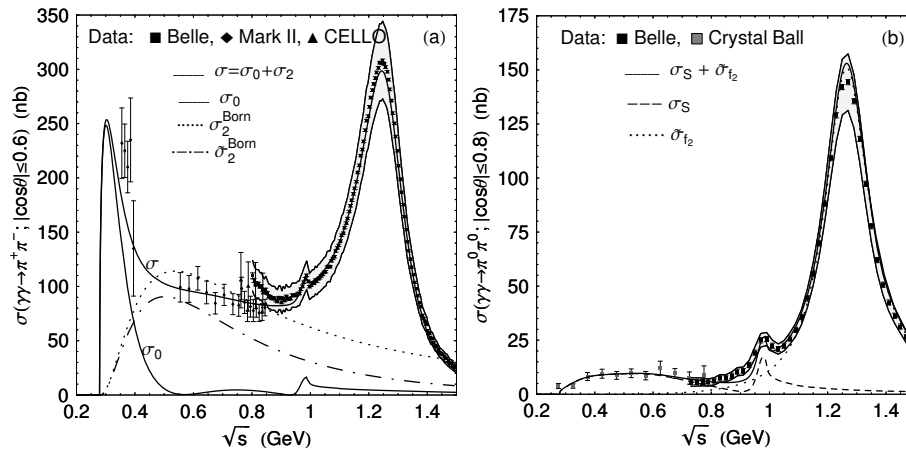


Fig. 11. The descriptions of the Belle data on $\gamma\gamma \rightarrow \pi^+\pi^-$ (a) and on $\gamma\gamma \rightarrow \pi^0\pi^0$ (b).

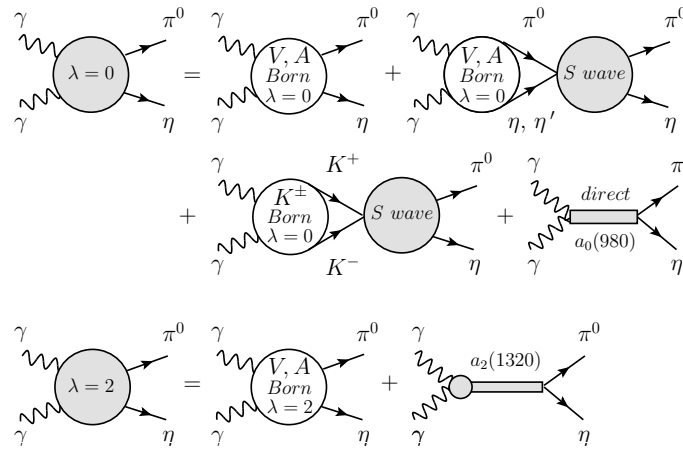


Fig. 12. Diagrammatic representation for the helicity amplitudes $\gamma\gamma \rightarrow \pi^0\eta$.

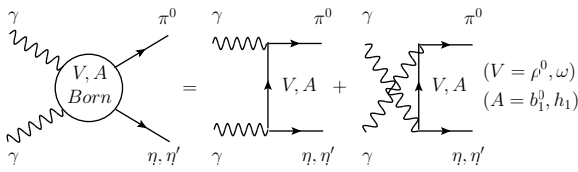


Fig. 13. The Born sources for $\gamma\gamma \rightarrow \pi^0\eta$.

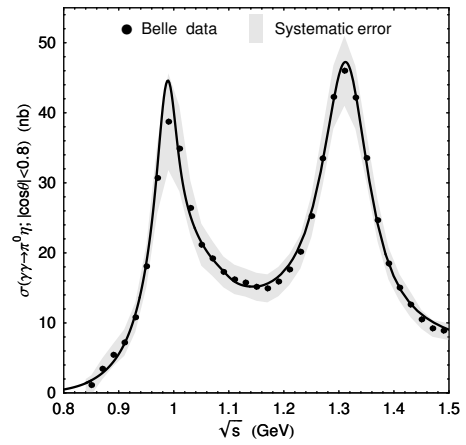


Fig. 14. The description of the Belle data on $\gamma\gamma \rightarrow \pi^0\eta$.

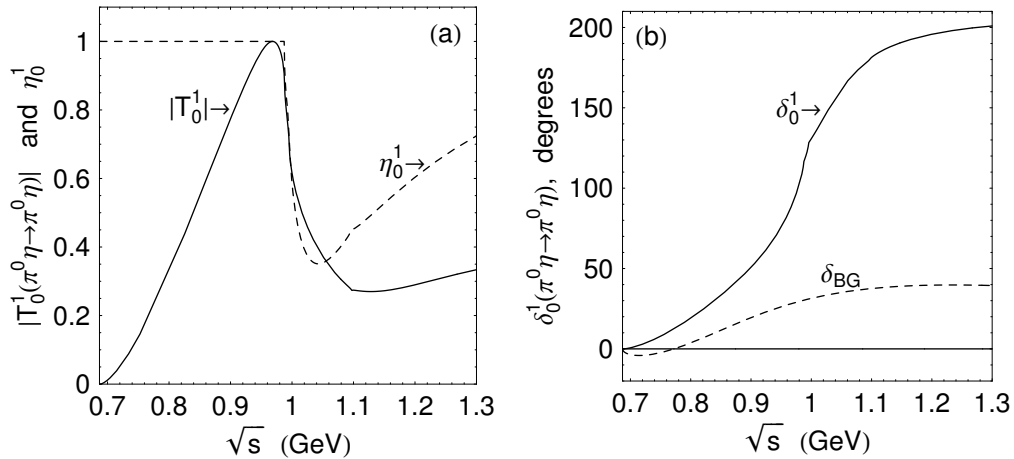


Fig. 15. Preliminary results for the $\pi^0\eta \rightarrow \pi^0\eta$ reaction amplitude.

19 Summary

The mass spectrum of the light scalars, $\sigma(600)$, $\kappa(800)$, $f_0(980)$, $a_0(980)$, gives an idea of their $q^2\bar{q}^2$ structure.

Both intensity and mechanism of the $a_0(980)/f_0(980)$ production in the radiative decays of $\phi(1020)$, the $q^2\bar{q}^2$ transitions $\phi \rightarrow K^+K^- \rightarrow \gamma[a_0(980)/f_0(980)]$, indicate their $q^2\bar{q}^2$ nature.

Both intensity and mechanism of the scalar meson decays into $\gamma\gamma$, the $q^2\bar{q}^2$ transitions, $\sigma(600) \rightarrow \pi^+\pi^- \rightarrow \gamma\gamma$, $f_0(980)/a_0(980) \rightarrow K^+K^- \rightarrow \gamma\gamma$, indicate their $q^2\bar{q}^2$ nature also.

In addition, the absence of $J/\psi \rightarrow \gamma f_0(980)$, $a_0(980)\rho$, $f_0(980)\omega$ in contrast to the intensive $J/\psi \rightarrow \gamma f_2(1270)$, $\gamma f_2'(1525)$, $a_2(1320)\rho$, $f_2(1270)\omega$ decays intrigues against the P wave $q\bar{q}$ structure of $a_0(980)$ and $f_0(980)$ also.

References

- 1 Achasov N N, Shestakov G N. Phys. Rev. D, 1994, **49**: 5779–5784
- 2 Achasov N N, Shestakov G N. Phys. Rev. Lett., 2007, **99**: 072001
- 3 Caprini I, Colangelo G, Leutwyler H. Phys. Rev. Lett., 2006, **96**: 132001
- 4 Jaffe R L. Phys. Rev. D, 1977, **15**: 267–280, 281–289
- 5 Achasov N N, Devyanin S A, Shestakov G N. Phys. Lett. B, 1982, **108**: 134–139; Z. Phys. C, 1982, **16**: 55–64
- 6 Achasov N N, Kiselev A V. Phys. Rev. D, 2006, **73**: 054029
- 7 Achasov N N, Ivanchenko V N. Nucl. Phys. B, 1989, **315**: 465–476; Achasov N N, Gubin V V. Phys. Rev. D, 1997, **56**: 4084–4097; Phys. Rev. D, 2001, **63**: 094007; Achasov N N. Usp. Fiz. Nauk, 1998, **168**: 1257–1261 [Physics-Uspekhi, 1998, **41**: 1149–1153]; Nucl. Phys. A, 2003, **728**: 425–438; Achasov N N, Kiselev A V. Phys. Rev. D, 2003, **68**: 014006; Phys. Rev. D, 2006, **73**: 054029
- 8 Achasov N N, Devyanin S A, Shestakov G N. Z. Phys. C, 1985, **27**: 99–105; Achasov N N, Shestakov G N. Z. Phys. C, 1988, **41**: 309–317; Usp. Fiz. Nauk, 1991, **161**(6): 53–108 [Sov. Phys. Usp., 1991, **34**: 471–496]
- 9 Achasov N N, Shestakov G N. Phys. Rev. D, 2005, **72**: 013006; Phys. Rev. D, 2008, **77**: 074020; Pisma Zh. Eksp. Teor. Fiz., 2008, **88**: 345–350 [JETP Lett., 2008, **88**: 295–300]; Achasov N N. Invited Talk at The 15th International Seminar on High Energy Physics: Quarks-2008, Sergiev Posad, Russia, arXiv: 0810.2601 [hep-ph]; Achasov N N, Shestakov G N. arXiv: 0905.2017 [hep-ph]; Pisma Zh. Eksp. Teor. Fiz., 2009, **90**: 355–360; [JETP Lett., 2009, **90**: 313–318]
- 10 Mori T et al. Phys. Rev. D, 2007, **75**: 051101(R); J. Phys. Soc. Jap., 2007, **76**: 074102; Uehara S et al. Phys. Rev. D, 2008, **78**: 052004; Phys. Rev. D, 2009, **80**: 032001